

## Letter to the Editor

# The thermal and non-thermal gaseous halo of NGC 5775<sup>\*</sup>

R. Tüllmann<sup>1,2</sup>, R.-J. Dettmar<sup>2</sup>, M. Soida<sup>3</sup>, M. Urbanik<sup>3</sup>, and J. Rossa<sup>2</sup>

<sup>1</sup> European Southern Observatory, Karl-Schwarzschild-Strasse 2, 85748 Garching, Germany

<sup>2</sup> Ruhr-Universität Bochum, Astronomisches Institut, 44780 Bochum, Germany

<sup>3</sup> Jagiellonian University, Astronomical Observatory, 30-244 Krakow, Poland

Received 15 August 2000 / Accepted 2 October 2000

**Abstract.** In this letter we present first results from spectroscopic observations of Diffuse Ionized Gas (DIG) in the halo of NGC 5775 obtained with FORS1<sup>1</sup> attached to UT1/Antu of the Very Large Telescope (VLT). At our slit position perpendicular to the disk (41'' SE of the nucleus) the emission of [N II]λ6583, [O III]λ5007, and [O II]λ3727 is detected out to 9 kpc into the halo, allowing possible ionization mechanisms of the DIG to be examined. Photoionization models which assume a dilute radiation field are able to fit the data for the disk, but they cannot account for the line ratios measured in the halo (e.g., [O I]/Hα or [O II]/Hα). In particular they fail to predict the observed increase of [O III]λ5007/Hα with increasing  $|z|$ . The most striking result concerns the kinematics of the halo gas. Velocities at high galactic latitudes drop from the midplane value to reach the systemic velocity at  $z \approx 9$  kpc. An analysis of VLA archive data of the polarized radio-continuum emission at 4.86 GHz and 1.49 GHz reveals that magnetic fields in the halo have a strong component perpendicular to the disk and are aligned with the Hα and radio-continuum spurs in the halo. This can result either from a strong wind action or, more likely, from the generation of dipolar magnetic fields. We briefly discuss the interrelation of the magnetic field structure and gas dynamics, in particular the role of magnetic fields in gas outflows, as well as the possible heating of DIG by magnetic reconnection.

**Key words:** galaxies: halos – galaxies: individual: – galaxies: ISM – galaxies: kinematics and dynamics – galaxies: magnetic fields – galaxies: structure

### 1. Introduction

There is increasing evidence that halos of normal spiral galaxies contain a complex multiphase interstellar medium (ISM) (for a review see, e.g., Dahlem 1997). Besides a hot component as observed by X-ray emission ( $>10^6$  K) or UV absorption ( $\sim 0.5 \times 10^5$  K), Diffuse Ionized Gas (DIG) constitutes another

important phase of typically  $10^4$  K (Dettmar 1992). This component is easily observed by its H II region like line emission and is found to be widespread in galaxies with actively star forming disks (Rand 1996, Dettmar 1999, Rossa & Dettmar 2000).

In the last couple of years two important problems have been discussed with regard to the physics of this interstellar gas phase. The observed line ratios are not explained in a straight forward way by pure photoionization models and require additional heating mechanisms of the halo gas (e.g., Golla et al. 1996, Rand 1997, Tüllmann & Dettmar 2000) while first kinematic observations hint at a slower rotation of halo gas if compared to the underlying disk (Rand 1998). Both kinds of observations could help to constrain models of the origin of halo gas which in turn are important for the understanding of galaxy evolution since large scale mass flows are of influence for star formation and chemical evolution.

Only for a few objects, such as NGC 891 (Dahlem et al. 1994), NGC 4631 (Golla & Hummel 1994), and NGC 5775, the various components of the halo ISM are observed with sufficient sensitivity and resolution to study possible physical processes at their interfaces such as turbulent mixing or thermal conduction. For such processes yet another ISM component can be of importance, namely the non-thermal component consisting of magnetic fields and cosmic rays as observed by its radio-continuum radiation. Any large scale gas motion and in particular its  $z$ -component will also be of importance for dynamo theories which try to explain the large scale distribution of magnetic fields in galaxies. However, various approaches to describe galactic dynamos are still very controversial and more detailed information on galactic gas flows in halos as well as magnetic field structures could help constraining such models.

For all these questions, the case of the Sc edge-on galaxy NGC 5775 has received some attention recently, since marked radio-continuum (Duric et al. 1998) and H I (Irwin 1994) halo components are accompanied by a very extended DIG halo (Dettmar 1992, Collins et al. 2000) for which a strong decline of the rotational velocity with height above the plane ( $z$ ) has been found (Rand 2000).

In this letter we report on first spectroscopic results for the DIG halo of NGC 5775 with the VLT, confirming the strong

Send offprint requests to: rtuellma@eso.org

<sup>\*</sup> Based on observations collected at the European Southern Observatory, Paranal (Chile); Proposal N<sup>o</sup>: 63.N-0573(A)

$z$ -dependence of the halo rotation presented by Rand (2000), along with a first detailed determination of the magnetic field structure in the halo from VLA radio-continuum observations.

## 2. Observations

Spectroscopic observations were carried out with FORS1<sup>1</sup> at VLT/UT1 in longslit mode on 1999 June 14–15 at a median seeing of 0''.7. A Tek 2048 × 2046 CCD with a pixel size of 24 × 24 μm and a spatial resolution of 0''.2 pix<sup>-1</sup> was used for the measurements. Grism GRIS\_600B+12 was chosen for the blue and GRIS\_600R+14 for the red spectral region, yielding a wavelength coverage of 3500–5900 Å and 5250–7400 Å, respectively. The slit length of FORS1 is 6''.8 and the selected slit width of 1''.31 gives an average resolution of 5.9 Å for the red and 6.2 Å for the blue grism, respectively. Our slit covers large filamentary structures of H $\alpha$  emission in the NE and SW halo (Fig. 1). For each grism the total integration time amounted to 3 hours, reaching a noise level of  $1.26 \times 10^{-19}$  ergs cm<sup>-2</sup> s<sup>-1</sup> Å<sup>-1</sup> pix<sup>-1</sup>. Data reduction was performed in the usual manner using standard IRAF software while the analysis was done within the MIDAS environment.

Maps of total power and the linearly polarized radio-continuum emission of NGC 5775 at 1.49 GHz and 4.86 GHz have been obtained from archive data of the Very Large Array (VLA) of the National Radio Astronomy Observatory (NRAO<sup>2</sup>). All data were recorded during 1989–1994. The total observation time used on source was about 10 hours at 4.86 GHz (D-array), 14 hours at 1.49 GHz with C-array, and 2.5 hours with D-array. Data reduction has been performed with the AIPS software package following standard procedures. The r.m.s. noise obtained in the final maps is 16 μJy/b.a. and 100 μJy/b.a. in total power, and 7 μJy/b.a. and 25 μJy/b.a. in polarized intensity at 4.86 GHz and 1.49 GHz, respectively.

## 3. Results and discussions

### 3.1. Ionization

Several strong emission lines such as [N II]λ6583 or [O II]λ3727 can be traced out to 66'' or 9 kpc (assuming a distance of  $D = 26.7$  Mpc) above the disk in both directions, much further than any previous imaging result. Similar findings have been reported by Rand 2000 for the western part of NGC 5775. All measured line ratios are presented in Fig. 2. Some ratios, such as [S II] and [O I], are lower in the SW section, most likely due to a more patchy structure of the filament. With an inclination of  $i = 84^\circ$ , NGC 5775 is close to edge-on and inclination effects are considered to be negligible. In order to clarify the issue of possible ionization mechanisms of the DIG we compare our observational results with predictions of pure photoionization models from Mathis (1986, Ma86 hereafter) and Domgörgen & Mathis (1994, DM94 hereafter). If we adopt pho-

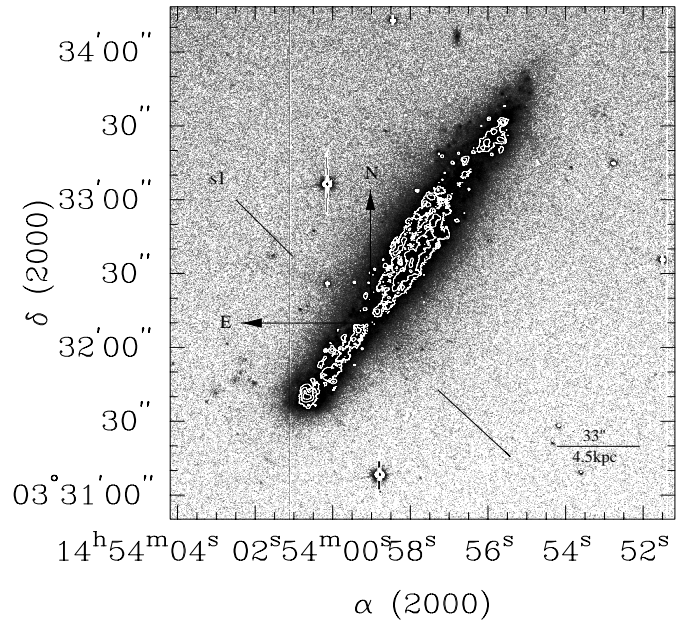


**Fig. 1.** Continuum subtracted H $\alpha$  image of NGC 5775 obtained with EMMI at the NTT. H $\alpha$ -contours shown for the disk reveal that s1 covers a gap of H $\alpha$  emission in the disk, cutting also through the NE and SW filament.

toionization by OB stars as the only ionization source and that radiation gets more and more dilute as it extends towards the halo, these models should reproduce observational data, such as the rising [O III]/H $\alpha$ , non-linear changes in [S II]/[N II], or extreme ratios of [O I]/H $\alpha$  and He I/H $\alpha$ .

[N II]/H $\alpha$  is fitted only for the disk by the model of Ma86 assuming a very soft radiation field ( $\log g = -6$ ) and O7 stars with effective temperatures of 35000 K as ionizing sources, whereas the DM94 model fails completely. By no means DM94 can reproduce halo ratios for [S II]/H $\alpha$  larger than 0.66, while Ma86 gives correct values ranging from 0.26 for the disk to 0.88 for the halo. Since these models predict an increase of [S II]/[N II] towards the halo, most likely a consequence of slightly different ionization potentials of S<sup>+</sup> and N<sup>+</sup>, they are unable to explain the non-linear trend visible in Fig. 2. Another important ratio is He I/H $\alpha$  which could be measured only close to the disk-halo interface of NGC 5775 ( $-1.1$  kpc  $< z < 1.65$  kpc), making this detection nevertheless unique concerning its  $z$  extent. However, both models underestimate this ratio by a factor of two.

The most striking feature in Fig. 2 is the rise of [O III]/H $\alpha$  with increasing  $z$  which is not explained by pure photoionization codes. Generally this ratio declines from values of about 2 in the disk to 0.8 in the halo.

Both models also fail to predict [O II]/H $\alpha$ . The lowest predicted values vary around 1, whereas the observed data never exceed this limit. [O I]/H $\alpha$  reveals with 0.33 for the SW and 0.48 for the NE halo by far the highest values ever measured for the DIG. Ma86 and DM94 are able to fit ratios only up to 0.1.

The extreme line ratios of He I/H $\alpha$  ( $> 0.05$ ) and [O I]/H $\alpha$  ( $> 0.3$ ), the shapes of [O III]/H $\alpha$  and [S II]/[N II] together with an unprecedented DIG extent of 9 kpc (see also Rand 2000)

<sup>1</sup> Focal Reducer/low dispersion Spectrograph

<sup>2</sup> NRAO is a facility of National Science Foundation operated under cooperative agreement by Associated Universities, Inc.

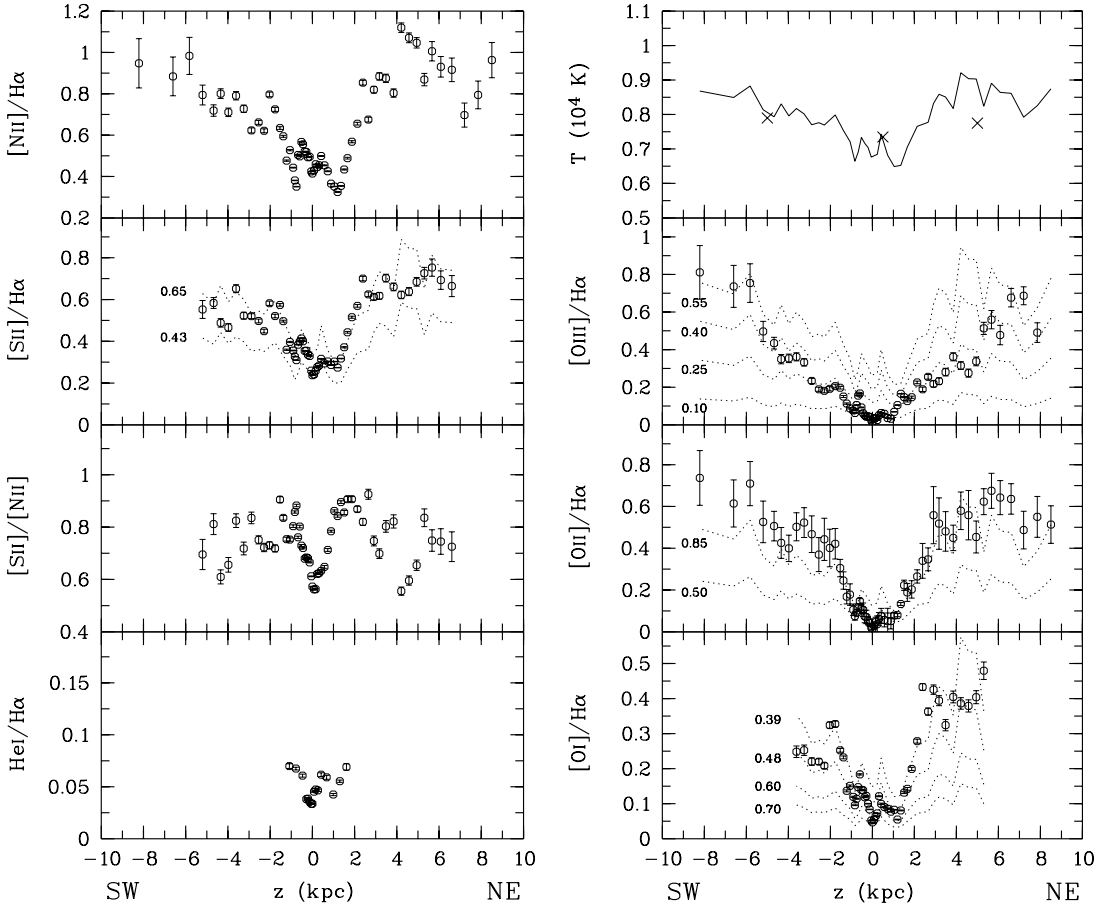


**Fig. 2.** Line ratios (corrected for interstellar extinction) plotted as a function of  $|z|$ . Theoretical line ratios (dotted lines) based on temperature profiles (measured from nitrogen emission, upper right) are fitted to the data by varying the corresponding ionization fraction. “x”-symbols are from temperature determinations using upper limits of  $[\text{N II}]\lambda 5755$  emission and are given as a consistency check.

make this galaxy the most outstanding and challenging test-bench for future ionization models.

Since common photoionization models are unable to reproduce the data for halo DIG in external galaxies as well as the Reynolds-layer of the Milky Way, recent studies (e.g., Rand 1998, Reynolds et al. 1999, Tüllmann & Dettmar 2000) have pointed out the need to involve additional ionization and/or heating mechanisms such as shocks, photoelectric heating by dust, or magnetic reconnection. These mechanisms should increase the electron temperature without affecting the ionization stage of an atom and dominate in the halo over collisional ionization. Following Haffner et al. (1999) and Collins & Rand (2000, CR hereafter) we used the  $[\text{N II}]\lambda 6583$  emission line to determine a temperature profile (shown in the upper right diagram of Fig. 2) which varies between 6500 and 9200 K. This profile can be used to derive theoretical line ratios (dotted lines in Fig. 2) for oxygen and sulfur. In order to fit the observed ratios, the ionization fraction as the only free parameter is changed accordingly. For consistency we also derived electron temperatures for the eastern part of NGC 5775 which are based on upper limits of the  $[\text{N II}]\lambda 5755$  emission line (Osterbrock, 1989). They have been estimated to be 7350 K in the disk (at 0.5 kpc), 7750 K for the NE filament, and 7900 K for the SW filament (both measured at

5.0 kpc), respectively. These values are in good agreement with our temperature determinations mentioned above and also with profiles obtained by CR for the central and western part of this galaxy.

Furthermore, plots on the right of Fig. 2 reveal prominent gradients which decrease as the ionization stage of oxygen increases. A likely physical reason could be a rising temperature towards the halo, according to Reynolds et al. (1999). This can simply be shown if we plot theoretical oxygen line ratios per ionization fraction vs. electron temperature. As a result  $[\text{O I}]/\text{H}\alpha$  increases much faster with  $T$  than  $[\text{O II}]/\text{H}\alpha$  or  $[\text{O III}]/\text{H}\alpha$ . Hence, different temperature dependencies of oxygen ionization stages are able to reflect the observed gradients.

### 3.2. Kinematics

The most surprising result revealed by our deep spectra concerns the kinematics of DIG at large  $z$ . The bright emission lines of hydrogen, nitrogen, and oxygen have been used to derive heliocentric velocities for the DIG as a function of  $z$  (vertical distance above the plane). As can be seen in Fig. 3 the gas velocity is with  $1822 \pm 8 \text{ km s}^{-1}$  highest at  $z = 0$  kpc and  $-1.6$  kpc, decreasing slowly towards larger  $z$  distances, finally reaching values close

or equal to the systemic velocity of  $1681 \text{ km s}^{-1}$  (Irwin 1994) at  $z = 9 \text{ kpc}$ . The measured trend is explainable assuming the DIG not to rotate at high galactic  $z$ . A similar result was recently reported by Rand (2000) for two different slit positions. This allows us to examine whether the halo DIG rotates regularly since our slit position and slit 1 of Rand (2000) both have a distance of  $45''$  from the center corresponding to  $6.1 \text{ kpc}$  but on opposite sides of the disk. The maximum rotational velocities at these positions (with respect to  $v_{\text{sys}}$  at  $z = 2 \text{ kpc}$ ) deviate only by  $4 \text{ km s}^{-1}$  and the dependence of  $v_{\text{rot}}(z)$  is to first order in agreement with a projected regular velocity field. However, different gradients imply that the kinematics of the DIG halo is more complex than a symmetric and static model would allow for. This requires more modelling including the shape of the dark matter potential and possible influences of outflow kinematics. The resolution of our spectra unfortunately is insufficient to check for the velocity dispersion of the lines.

Since our spectra have very high sensitivity at very good spatial resolution, Fig. 3 also indicates some small-scale structure in the velocity field with localized minima at  $z = -8.5, -4.0, 1.5, 5.2,$  and  $9.5 \text{ kpc}$ . Close to the disk, in particular in the NE, these changes can be explained by dust obscuration, “shifting” the peak velocity at the center to  $z = -1.6 \text{ kpc}$ . An R-band image of NGC 5775 gives evidence for large amounts of dust, mainly in the northern part, extending from the disk plane  $1.8 \text{ kpc}$  into the halo. The kinematical structures at larger  $z$  are not directly associated with observed dust features and hint at either an inhomogeneous DIG distribution along the line of sight or effects from flows.

### 3.3. Magnetic field structure in the halo of NGC 5775

In Fig. 4 we present maps of total power, polarized intensity, and apparent polarization B-vectors at  $4.86 \text{ GHz}$  overlaid upon an enhanced  $\text{H}\alpha$  image. NGC 5775 shows an extended radio envelope which can be traced beyond  $2 \text{ kpc}$  from the disk plane. While close to the disk plane the polarization B-vectors are generally disk parallel, at heights above  $1 \text{ kpc}$  they form a X-like pattern, corresponding also to similarly shaped extensions of polarized intensity.

Before discussing the magnetic field structure we make a comparison of the polarization information at both frequencies to estimate the possible influence of Faraday rotation and depolarization. For heights less than  $1 \text{ kpc}$  our estimates for a regular azimuthal magnetic field oriented parallel to the disk, assuming pressure balance with cosmic rays and typical thermal electron densities of  $0.03 \text{ cm}^{-3}$ , imply that NGC 5775 is Faraday thick at  $4.86 \text{ GHz}$  close to the disk plane. Therefore B-vector orientations are not conclusive. However, a reasonable agreement between the orientations of polarization angles at  $4.86 \text{ GHz}$  and  $1.49 \text{ GHz}$ , a relatively high polarization degree (reaching 30%) at  $4.86 \text{ GHz}$ , and the depolarization at  $1.49 \text{ GHz}$  by a factor of about  $0.3 - 0.4$  support the assumption that above  $1 \text{ kpc}$  the halo of NGC 5775 is Faraday-thin down to  $1.49 \text{ GHz}$ . Thus, if the B-vector orientations at two frequencies differ there locally by some tens of degrees, the rotation angle at

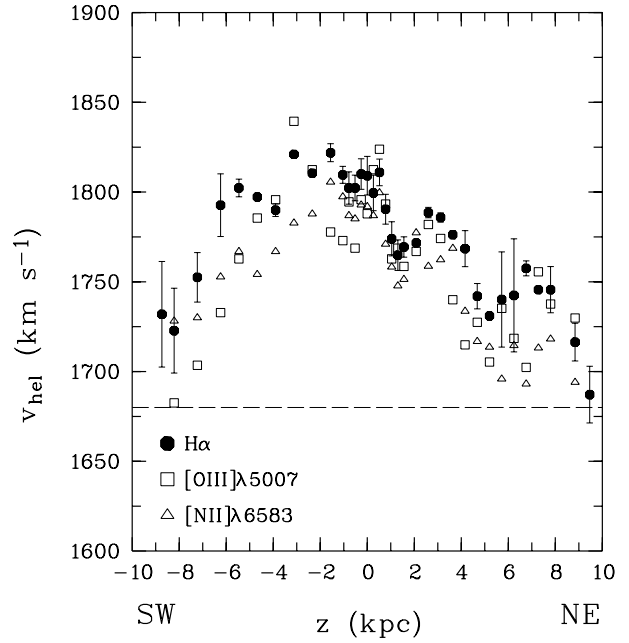


**Fig. 3.** Heliocentric velocities as a function of  $z$  for the minor slit s1. Dashed lines indicate the systemic velocity  $v_{\text{sys}}$  as measured by Irwin (1994). No qualitative differences are visible between the kinematical behavior of  $\text{H}\alpha$ ,  $[\text{O III}]\lambda 5007$ , and  $[\text{N II}]\lambda 6583$ .

$1.49 \text{ GHz}$  is smaller than  $90^\circ$ , hence the Faraday rotation bias at  $4.86 \text{ GHz}$  does not exceed  $10^\circ$ . However, in the SW part of the halo ( $\text{R.A.}_{2000} = 14^{\text{h}}53^{\text{m}}54^{\text{s}} \text{ Dec}_{2000} = +03^\circ33'15''$ ), similar orientations of B-vectors at both frequencies are apparently in conflict with the depolarization at  $1.49 \text{ GHz}$  by a factor of  $0.1$ , which raises the suspicion that it might be Faraday-thick. On the other hand numerical simulations show that this depolarization can also be due to pure Faraday dispersion in random fields, without substantial Faraday rotation.

From the above comparison we conclude that the observed B-vectors at  $4.86 \text{ GHz}$  in the halo at heights  $|z| > 1 \text{ kpc}$  are not significantly affected by Faraday rotation and that therefore the magnetic field in the halo has a significant vertical component. Such a vertical magnetic field component strong enough to be seen in emission can be generated in two ways. A spherically blowing galactic wind could result in an enhanced vertical component of the magnetic field. While the poloidal magnetic field preserves its quadrupole symmetry, resulting in B-vectors parallel to the plane below  $z \simeq 1 \text{ kpc}$ , characteristic X-shaped structures develop at larger heights (Brandenburg et al. 1993).

An alternative way to obtain the vertical B-vectors is the generation of the dipolar (called A-type) poloidal magnetic field produced by the dynamo process. The principal condition is a rigid rotation extending over a substantial range of galactocentric radius and a large vertical scaleheight of the ionized gas, both being true for NGC 5775 (Lehnert & Heckman 1996). In this case the B-component parallel to the disk would vanish. Unfortunately, this way of distinguishing both mechanisms cannot be used here because of the strong Faraday effects close to the disk. However, we note that the detailed analysis of Faraday ro-

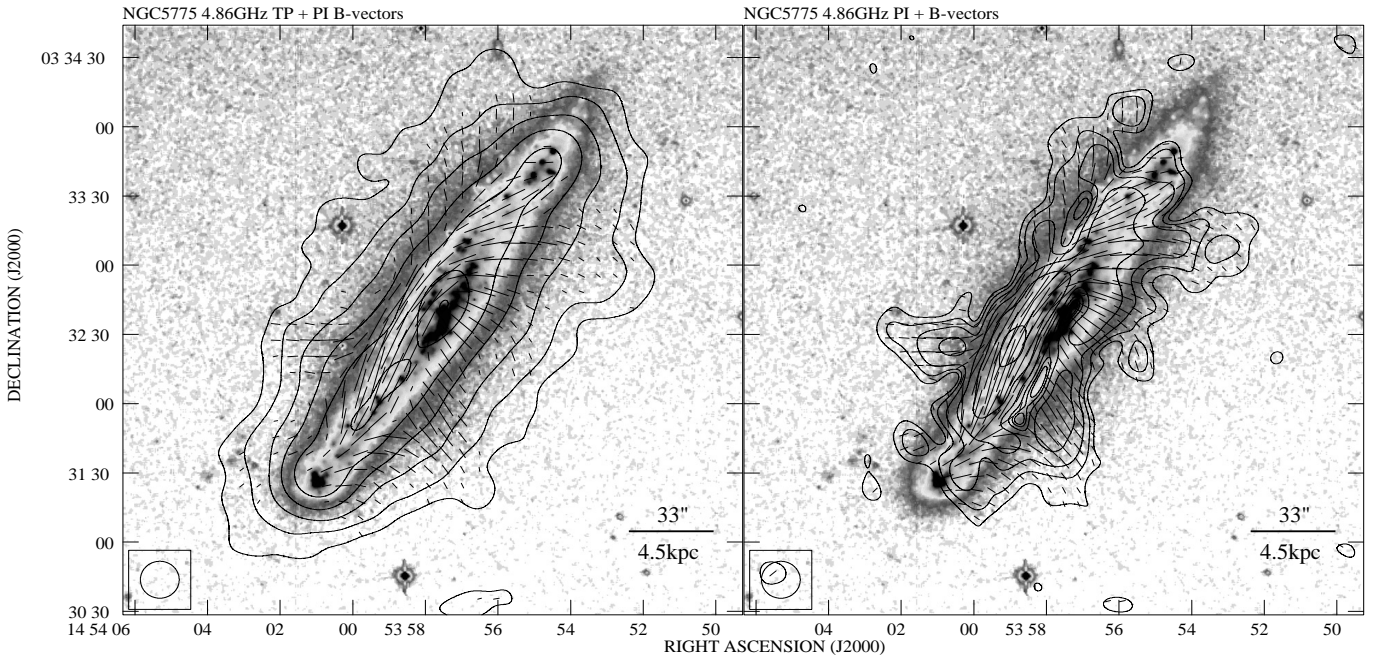


**Fig. 4.** VLA radio-continuum maps with total power (left), polarized intensity (right) and resulting B-vectors overlaid on a  $H\alpha$  image of NGC 5775. Contours are at  $3, 8, 21, 55, 144, 377,$  and  $610 \times 16 \mu\text{Jy}/\text{beam}$  for TP and  $3, 5, 8, 13, 21,$  and  $34 \times 7 \mu\text{Jy}/\text{beam}$  for PI, for the B-vectors a length of  $1''$  corresponds to  $10 \mu\text{Jy}$ .

tation angles reveals field reversals across the plane (excluding  $z < 1 \text{ kpc}$ ) in favour of a dipolar poloidal field.

Whether a vertical decrease of rotational speed, as seen in Fig. 3, makes this field mode growing faster remains yet to be investigated but cannot be excluded. We note that the existing dynamo models which account for rotation speed falling with  $z$  yield very different results. While little effect of vertical rotation decrease upon the dynamo efficiency was obtained for a classical dynamo concept (Brandenburg et al. 1993) a special model of a supernova-driven dynamo by Ferrière & Schmitt (2000) fails in this case to generate any stable, growing magnetic field mode. The dynamo models in case of a vertical rotation drop-off can be validated if only more information on the magnetic field structure in halos along with kinematical information would be available.

However, as noted by Collins et al. (2000) we need to consider the influence of the vertical magnetic field structure on the cosmic ray propagation and the gas flows. To clearly demonstrate the correlation of the radio-continuum spurs with the magnetic field structure we have applied a median filter to the total power map at 1.49 GHz, which revealed structural components inclined to the galaxy plane in the same X-shaped manner as the polarization B-vectors (Fig. 5).

The polarization features are anchored in the disk plane with the SE one being attached to a local radio bright region in the disk, most likely a star forming region. The total power spur at  $\text{R.A.}_{2000} = 14^{\text{h}}53^{\text{m}}53^{\text{s}}.1$ ,  $\text{Dec}_{2000} = +03^{\circ}32'55''$  curves towards south in its outer part; the same behaviour is seen for the polarization vectors at both frequencies. We suspect that they are associated with cosmic ray electron streaming from

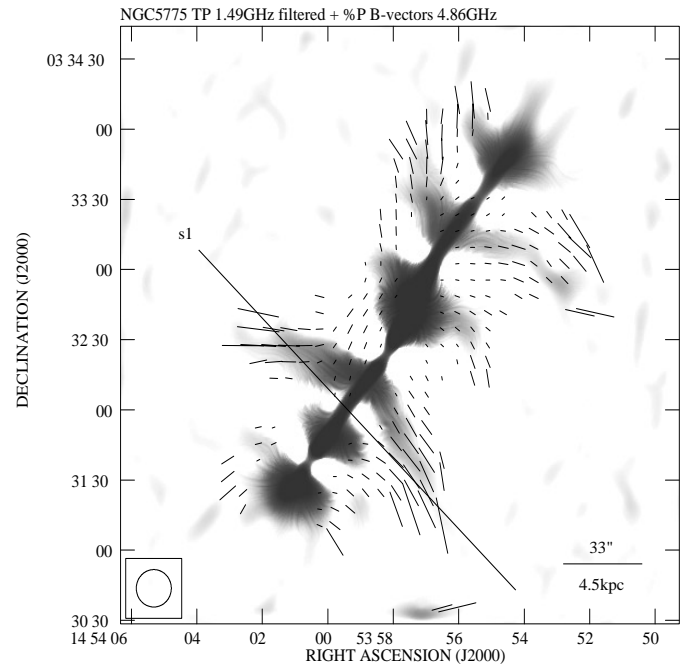


**Fig. 5.** The strongly filtered total power image of NGC 5775 at 1.49 GHz with a median filter applied. It shows in detail the loci of brightness maxima in the distribution of the total power brightness.

intensively star-forming regions along the inclined magnetic lines. The inclined spurs extend down to the disk plane which allows us to speculate that magnetic lines may do the same, as expected for the A-mode. We also note that the cosmic ray

propagation along the magnetic lines of the regular field may yield an X-shaped distribution of the polarized intensity (Fig. 4). Similarly, an easier streaming of the ionized gas along magnetic fields of the discussed geometry can give rise to the occurrence of H $\alpha$ -emitting spurs coincident with the radio ones and to an increased vertical scale of ionized gas in regions of magnetic structures highly inclined to the disk plane.

Finally we want to address the question whether the energy stored in the magnetic field could in principal help solving the heating problem discussed in Sect. 3.1. Magnetic reconnection as a heat source for DIG was suggested earlier, e.g., by Birk et al. (1998) or Reynolds et al. (1999), the latter based on an analogy from solar physics proposed by Raymond (1992). In the following we use the heating rate for magnetic reconnection  $G_{\text{mag}}$  as derived by Lesch & Bender (1990):  $G_{\text{mag}} = B^2 v_A / 8\pi L$ , with  $v_A$  the Alfvén velocity and  $L$  the dissipation length. For characteristic regions in the spurs the minimum total magnetic field strength implied by the pressure balance with cosmic rays is  $\geq 5 \mu\text{G}$ . With this value we obtain the required heating rates as determined by Reynolds et al. (1999) for DIG densities of typically  $n_e = 10^{-3} \text{ cm}^{-3}$  if  $L$  is in the order of parsec, not unreasonable for structures in the ISM. Since this heating rate depends on the Alfvén velocity and thus on  $n_e^{-1/2}$  the increasing importance of the additional heating source with decreasing particle density would be a natural consequence. Reconnection could also be responsible for the growth of ordered magnetic field structures in the spurs. It has been suggested that this process could help to reorganize the field structure in a galactic fountain flow (e.g., Kahn 1991).

#### 4. Summary and conclusions

The most important results can be summarized as follows:

- emission lines of DIG can be traced out to 9 kpc in the halo of NGC 5775
- the rotational velocity of the DIG drops from the rotational value at the midplane and approaches the systemic velocity at distances  $z > 6.0$  kpc
- pure photoionization models are unable to reproduce the extreme line ratios of [O I]/H $\alpha$ , He I/H $\alpha$ , and [O III]/H $\alpha$  as measured for the halo
- a high degree of polarization and a strong vertical component of the magnetic field are observed in the halo. We found some, yet weak evidence for the dipolar magnetic field
- a correlation exists between extraplanar DIG and magnetic fields, evidenced by the alignment of magnetic B-vectors with prominent halo features in the DIG and radio-continuum distribution

- we suggest that reconnection processes play a substantial role in both heating the DIG structures in the halo and building up regular fields away from the disk plane

*Acknowledgements.* RT acknowledges support through the ESO Studentship Programme. Research in this field is supported through grant 50 OR 9707 from DLR at Ruhr-University and through grant no. PB4264/P03/99/17 from Polish Research Committee (KBN) at Jagiellonian University. The project also benefitted from the exchange programme between both universities. We thank the referee for asking the right questions and RJD appreciates valuable discussions with H. Lesch and A. Shukurov on the role of magnetic fields for the physics of the ISM.

#### References

- Birk G. T., Lesch H., Neukirch T., 1998, MNRAS 296, 165  
 Brandenburg A., Donner K. J., Moss D., Shukurov A., Sokoloff D. D., Tuominen I., 1993, A&A 271, 36  
 Collins J. A., Rand R. J., Duric N., Walterbos R. A. M., 2000, ApJ 536, 645  
 Collins J. A., Rand R. J., 2000, in: “Gas & Galaxy Evolution”, (eds.) J. Hibbard et al., ASP Conf. Ser., in press  
 Dahlem M., 1997, PASP 109, 1298  
 Dahlem M., Dettmar R.-J., Hummel E., 1994, A&A 290, 384  
 Dettmar R.-J., 1992, Fund. Cosm. Phys. 15, 143  
 Dettmar R.-J., 1999 in: “The Physics and Chemistry of the Interstellar Medium”, (eds.) V. Ossenkopf et al., GCA-Verlag Herdecke, p. 18  
 Domgörgen H., Mathis J.S., 1994, ApJ 428, 647  
 Duric N., Irwin J., Bloemen, H., 1998, A&A 331, 428  
 Ferrière K., Schmitt, D., 2000, A&A 358, 125  
 Golla G., Hummel E., 1994, A&A 284, 777  
 Golla G., Dettmar, R.-J., Domgörgen, H., 1996, A&A 313, 439  
 Haffner L.M., Reynolds R.J., Tufte S.L., 1999, ApJ 523, 223  
 Irwin J. A., 1994, ApJ 429, 618  
 Kahn F. D., 1991, in: IAU Symp. 144 “The Interstellar Disk-Halo Connection”, ed. H. Bloemen, Kluwer, p. 1  
 Lehnert M. D., Heckman T. M., 1996, ApJ 472, 546  
 Lesch H., Bender R., 1990, A&A 233, 391  
 Mathis J. S., 1986, ApJ 301, 423  
 Osterbrock D.E., 1989, “Astrophysics of Gaseous Nebulae and Active Galactic Nuclei”, University Science Books  
 Rand R. J., 1996, ApJ 462, 712  
 Rand R. J., 1997, ApJ 474, 129  
 Rand R. J., 1998, ApJ 501, 137  
 Rand R. J., 2000, ApJ 537, L13  
 Raymond J. C., 1992, ApJ 384, 502  
 Reynolds R. J., Haffner L. M., Tufte S. L., 1999, ApJ 525, L21  
 Rossa J., Dettmar R.-J., 2000, A&A 359, 433  
 Tüllmann R., Dettmar R.-J., 2000, A&A (in press)